

## CHAPTER 4

### MULTISCALE MODELLING AND SIMULATION OF 3D BRAIDED COMPOSITES WITHOUT USING CNTs

#### 4.1. Unit-Cell Model (Without CNTs)

A unit-cell is defined as a cell or a building block of a composite. It is also called a representative volume element (RVE). A unit-cell as the name suggests describes a unit portion of a composite material which when stacked together in rows and columns will form the actual composite structure. For example, a unit cell of a simple particulate composite is a cube with a spherical particle at the centre. A unit-cell model is defined in terms of the micro structural parameters including volume fractions, connectivity, and anisotropic spatial distribution of phases. One of the key issues in estimation of the effective constitutive relation of a composite is the appropriate modelling of the stress transfer relation of the constituent phases with specific microstructures.

In this paper, a unit cell model having the structure of 3D full-five directions is shown in **Figure 4.1**, where  $a$ ,  $b$  and  $c$  are width, thickness and height of the unit-cell respectively. An interior angle is the angle between central axis of the braiding yarn and  $Z_0$  axis. For the geometrical modelling of the unit-cell, two assumptions have been made; braiding and axial yarns are assumed to be straight with circular cross-sections of same diameters. Under these assumptions, the final position of each carrier in the unit-cell can be selected as shown in **Figure 4.2**. To prepare finite element model of the unit-cell for further analysis, the size of the unit-cell (**Figure 4.1**) in the composite is taken as follows (**Table 4.1**).

**Table 4.1:** Dimension of unit-cell

Parameters	Value
Width ( $a$ )	20 mm
Thickness ( $b$ )	20 mm
Height ( $c$ )	20 mm
Interior angle	35.6°

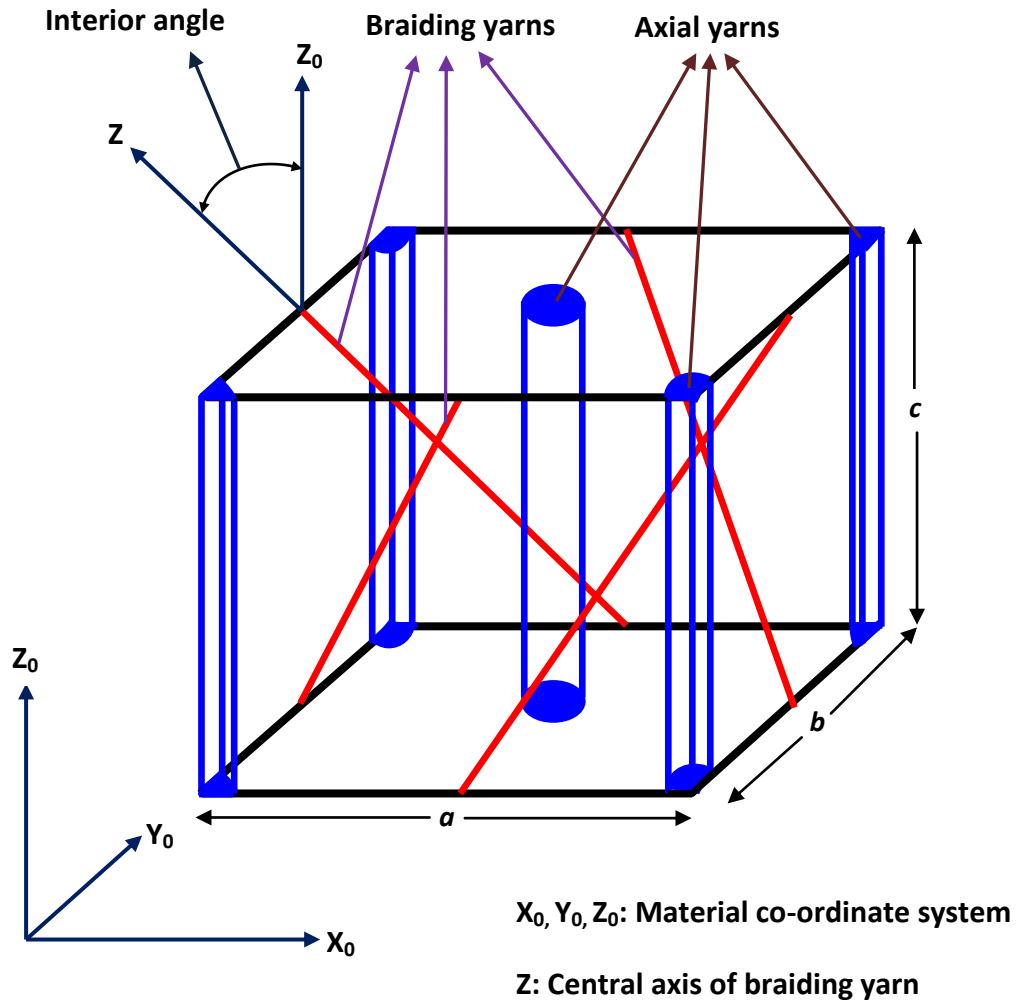


**Figure 4.1:** Schematic illustration of the fiber structure of 3D full five-directional braided composites

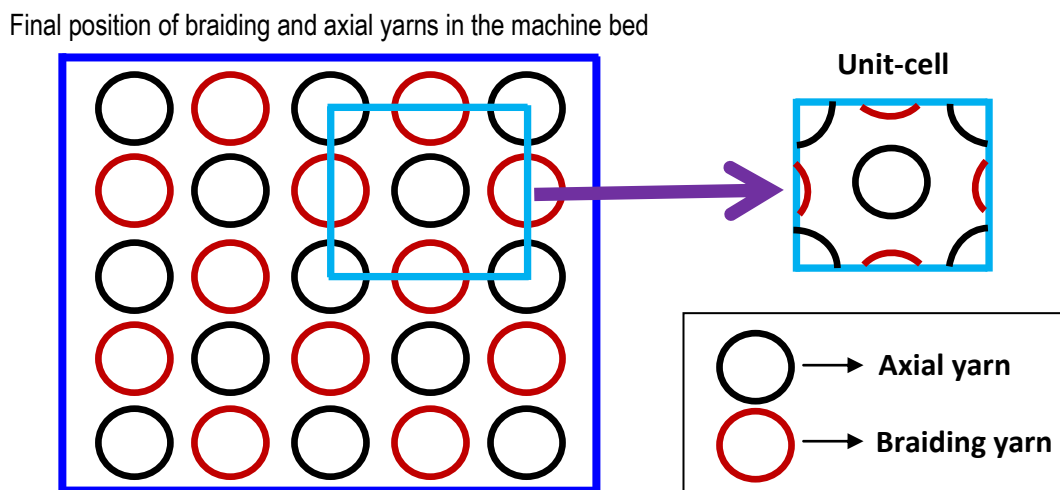


**Figure 4.2:** Selection of the unit-cell of 3D full five-directional braided composites

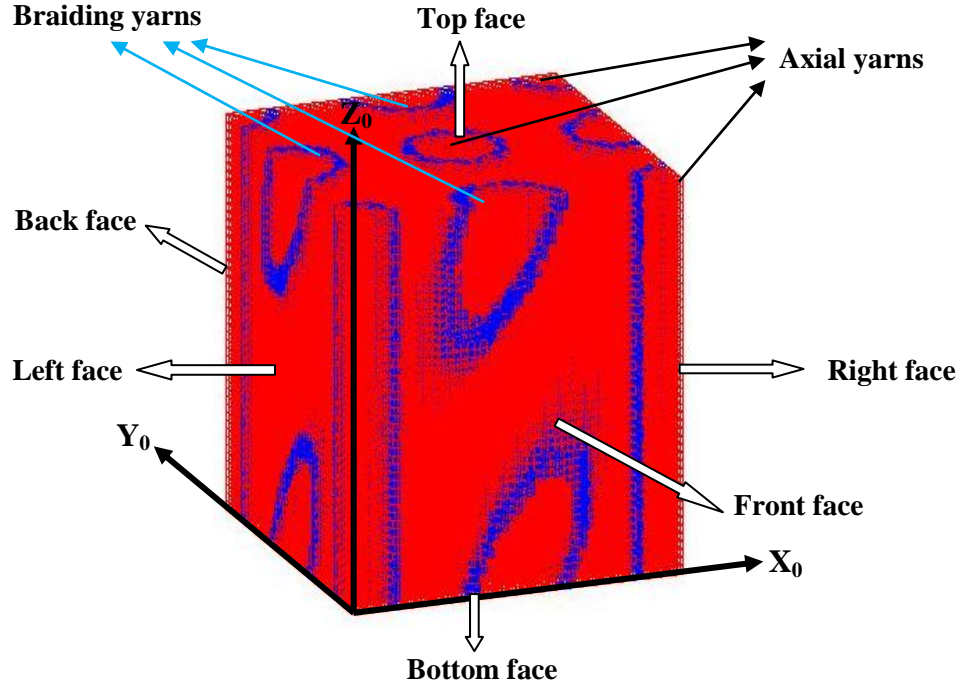


**Figure 4.3:** 3D Unit-cell model for 3D full five directional braided composite

In the present work, the 3D full five-directional braided composite has been modelled as shown in **Figure 4.3**. An algorithm is developed to simulate the different dynamics of 3D full five-directional braided composites so that one can understand, and design new composites with an ease. The fibers in the microstructure are assumed as 3D solid cylindrical inclusions. The matrix and the reinforcement both are in connection with the homogenous medium which approximates the intertwining structure of the 3D braided composite. The radius of each fiber is determined using fiber volume fraction. Following relation is used to calculate the radius of the fiber:

$$V_f = \frac{V_y}{V} \quad (4.1)$$

where,  $V_f$  is the fiber volume fraction,  $V_y$  is the total volume of the yarns (axial and braiding)  $= n \times (\pi r^2 h)$ ,  $V$  is the volume of the unit-cell,  $r$  is radius of the fiber,  $h$  is the height of the fiber,  $n$  is number of fibers in the unit-cell. The fibers are used to form nine level set values for each node in the domain. These values are the normal distances from the boundary (Chessa *et al.*, 2002), and are given by

$$\psi(X_0, Y_0, Z_0) = \sqrt{x^2 + y^2 + z^2} - r_c \quad (4.2)$$

where,  $x, y, z$  are co-ordinates of centre of the cylindrical inclusion (fiber),  $r_c$  is the radius of the solid cylinder (fiber),  $\psi$  is level set function.

#### 4.2. Effective Medium Approximation

It has been noticed that the different 3D braided composites show different mechanical properties depending on the volume fraction, ratios of elastic modulus, interior angle, geometry, etc. Thus, homogenization of these composite is very important to analyse and characterise their mechanical behaviour. The effective medium approximation (EMA) suggests that an equivalent homogenous medium can be found out, which will have properties similar to that of composite i.e. by replacing the actual heterogeneous composite by an equivalent homogeneous material. This homogenous material is an idealization but is an essential approximation for the further analysis of the composite, which otherwise is very difficult to analyse. In past, many researchers have used EMA approach to evaluate the effective properties of the composites. In fact, the study of composite materials involves the finding of the effective properties such as Young's modulus, shear modulus, Poisson's ratio, etc. Thus, EMA is very relevant and useful technique to find out the effective properties of a composite. There are various methods through which we can find out a homogenous material, which would mimic the properties of the composite material. To approximate a medium we have to first find that property which influences the overall property. For example, volume fraction is the most important factor, which influences a composite material. Other factors like geometry, interior angle, and temperature also affects the overall effective properties of the composite.

In the present work, 3D full five directional braided composite has been solved using XFEM, and analyzed by EMA. This composite shows transversely-isotropic behaviour at macroscopic level due to its fiber orientation in a particular direction. In this composite, both the matrix and the fibers are assumed to be isotropic in nature. A homogenization approach is used to obtain the effective elastic properties of 3D full five-directional braided composites by considering the heterogeneous behavior at micro-scale and homogeneous behavior at macro-scale (Xu and Xu, 2008).

In general, the global strain–stress relation can be written as

$$\bar{\varepsilon}_i = S_{ij} \bar{\sigma}_j \quad (4.3)$$

where,  $S_{ij}$  is the effective compliance matrix. Assuming a set of the global stress,  $\bar{\sigma}_{ij}$  and applying the essential boundary conditions given in **Table 4.2**, one can obtain a strain

distribution of the RVE. Then, the global strain,  $\bar{\varepsilon}_{ij}$  corresponding to global stress can be obtained by  $\bar{\varepsilon}_{ij} = \frac{1}{V} \int_V \varepsilon_{ij} dV$  where,  $V$  is the volume of the unit-cell.

**Table 4.2:** Boundary condition for calculation of effective elastic properties of the unit-cell

Cases	Properties	Essential boundary condition	Natural boundary condition
1	$E_x$	$u_x = 0$ (on left face), $u_y = 0$ (on front & back face), $u_z = 0$ (on bottom & top face),	axial stress along $X_0$ (on right face)
2	$E_y$	$u_x = 0$ (on left & right face), $u_y = 0$ (on back face), $u_z = 0$ (on bottom & top face),	axial stress along $Y_0$ (on front face)
3	$E_z$	$u_x = 0$ (on left & right face), $u_y = 0$ (on front & back face), $u_z = 0$ (on bottom face),	axial stress along $Z_0$ (on top face)
4	$G_{xz}$	$u_x = u_y = 0$ (on bottom & top face), $u_x = u_z = 0$ (on back face), $u_x = 0$ (on front face), $u_y = u_z = 0$ (on left & right face),	shear stress along $Z_0$ (on front face)
5	$G_{yz}$	$u_x = u_y = 0$ (on bottom & top face), $u_x = u_z = 0$ (on front & back face), $u_y = u_z = 0$ (on left face), $u_z = 0$ (on right face),	shear stress along $Y_0$ (on right face)
6	$G_{xy}$	$u_x = u_y = 0$ (on bottom face), $u_y = 0$ (on top face), $u_x = u_z = 0$ (on front & back face), $u_y = u_z = 0$ (on left & right face),	shear stress along $X_0$ (on top face)

**Table 4.3:** Loading case of natural boundary condition

K	$\bar{\sigma}_x(N)$	$\bar{\sigma}_y(N)$	$\bar{\sigma}_z(N)$	$\bar{\tau}_{xz}(N)$	$\bar{\tau}_{yz}(N)$	$\bar{\tau}_{xy}(N)$
1	100	0	0	0	0	0
2	0	100	0	0	0	0
3	0	0	100	0	0	0
4	0	0	0	100	0	0
5	0	0	0	0	100	0
6	0	0	0	0	0	100

In above boundary conditions,  $u_x$ ,  $u_y$  and  $u_z$  denote the displacements in  $X_0$ ,  $Y_0$  direction and  $Z_0$  directions respectively. Thus, by applying six components of  $\bar{\sigma}_{ij}$  as presented in **Table 4.3**, six equations can be obtained. By assigning the six sets of the global stress,  $\bar{\sigma}_{ij}^k$  ( $k=1, 2 \dots 6$ ), the corresponding global strain  $\bar{\varepsilon}_{ij}^k$  can be calculated and the following equations can be obtained

$$\{\bar{\varepsilon}_i^1, \bar{\varepsilon}_i^2, \dots, \bar{\varepsilon}_i^5, \bar{\varepsilon}_i^6\} = S_{ij} \{\bar{\sigma}_j^1, \bar{\sigma}_j^2, \dots, \bar{\sigma}_j^5, \bar{\sigma}_j^6\} \quad (4.4)$$

Hence by solving the above equations, we can directly obtain the effective compliance matrix  $S_{ij}$  in the following form:

$$S_{ij} = \begin{bmatrix} \frac{1}{E_x} & -\frac{\nu_{xy}}{E_y} & -\frac{\nu_{xz}}{E_z} & 0 & 0 & 0 \\ -\frac{\nu_{yx}}{E_x} & \frac{1}{E_y} & -\frac{\nu_{yz}}{E_z} & 0 & 0 & 0 \\ -\frac{\nu_{zx}}{E_x} & -\frac{\nu_{zy}}{E_y} & \frac{1}{E_z} & 0 & 0 & 0 \\ 0 & 0 & 0 & \frac{1}{G_{xz}} & 0 & 0 \\ 0 & 0 & 0 & 0 & \frac{1}{G_{yz}} & 0 \\ 0 & 0 & 0 & 0 & 0 & \frac{1}{G_{xy}} \end{bmatrix} \quad (4.05)$$

### 4.3 Results and Discussion

The elastic properties of constituents of the composite in the unit-cell are listed in **Table 4.4**. The fiber-volume fraction of yarn is assumed to be 45% in the model. The XFEM mesh for the unit-cell consists of 8,000 nodes and 6,859 eight-noded brick elements.

**Table 4.4:** Mechanical properties of component materials

Materials	Young's modulus $E$ , GPa	Poisson's ratio ( $\nu$ )
<b>Carbon fiber T300</b>	221	0.3
<b>Epoxy resin</b>	4.5	0.3

After assigning the above mechanical properties to the component materials, the effective compliance matrix of the 3D full five-directional braided composite is evaluated and given as follows:

$$S_{ij} = \begin{bmatrix} 0.0310 & -0.0093 & -0.0063 & 0 & 0 & 0 \\ -0.0093 & 0.0310 & -0.0063 & 0 & 0 & 0 \\ -0.0063 & -0.0063 & 0.0211 & 0 & 0 & 0 \\ 0 & 0 & 0 & 0.0685 & 0 & 0 \\ 0 & 0 & 0 & 0 & 0.0685 & 0 \\ 0 & 0 & 0 & 0 & 0 & 0.0807 \end{bmatrix}_{GPa^{-1}} \quad (4.6)$$

It is noted that relatively fine mesh is required in order to obtain more accurate stress distribution, especially near the boundaries of the RVE.

According to the relationship between the elastic constants and the compliance matrix  $S_{ij}$ , nine independent elastic constants of 3D full five-directional braided composites can be

calculated by the following relations  $E_x = \frac{1}{S_{11}}$ ,  $E_y = \frac{1}{S_{22}}$ ,  $E_z = \frac{1}{S_{33}}$ ,  $\nu_{xy} = -\frac{S_{12}}{S_{22}}$ ,

$\nu_{xz} = -\frac{S_{13}}{S_{33}}$ ,  $\nu_{yz} = -\frac{S_{23}}{S_{33}}$ ,  $G_{xz} = \frac{1}{S_{44}}$ ,  $G_{yz} = \frac{1}{S_{55}}$ ,  $G_{xy} = \frac{1}{S_{66}}$ . **Table 4.5** gives the predicted

results for the unit-cell.

**Table 4.5:** Effective elastic constants predicted by XFEM

Young's Modulus (GPa)			Shear Modulus (GPa)			Poisson's ratio		
$E_x$	$E_y$	$E_z$	$G_{xz}$	$G_{yz}$	$G_{xy}$	$\nu_{xz}$	$\nu_{yz}$	$\nu_{xy}$
<b>32.21</b>	<b>32.21</b>	<b>47.39</b>	<b>14.60</b>	<b>14.60</b>	<b>12.39</b>	<b>0.3</b>	<b>0.3</b>	<b>0.3</b>

The unit cell of 3D full five-directional braided composites produced by the four-step 1×1 rectangular braiding procedure (**Figure 4.2**) is shown in **Figure 4.3**. The effect of fiber volume fraction under a same interior angle on the effective elastic properties of 3D full five-directional braided composites is studied. The upper bound and lower bound of the unit-cell for a particular fiber volume fraction can be calculated using rule of mixture as given below:

$$E_u = (V_f \times E_f) + (V_m \times E_m) \quad (4.7)$$

$$E_l = \frac{E_f \times E_m}{(V_f \times E_m) + (V_m \times E_f)} \quad (4.8)$$

where,  $E_u$  is the upper bound (axial modulus) of composite,  $E_l$  is the lower bound (transverse modulus) of composite,  $E_f$  is the elastic modulus of fiber (Carbon),  $E_m$  is the elastic modulus of matrix (Epoxy),  $V_f$  is the fiber volume fraction in the unit-cell and  $V_m$  is the matrix volume fraction in the unit-cell.

**Figure 4.4** describes the variation of  $E_z$  with the fiber volume fraction. This figure shows that the elastic modulus  $E_z$  increases sharply with the increase in fiber-volume fraction and lies within the theoretical bounds i.e. upper and lower bounds calculated by Eq. (4.7) and Eq. (4.8). **Figure 4.5** presents the variation of elastic moduli  $E_x (= E_y)$  with the fiber-volume fraction. These results show that with the increase in fiber-volume fraction, the elastic modulus  $E_x$  also increases. **Figures 4.6** and **4.7** show the variation of the shear modulus,  $G_{xy}$  and  $G_{xz} (G_{xz} = G_{yz})$  with the fiber volume fraction. From the results presented in these figures, it is seen that shear moduli increase monotonically with the increase in fiber-volume fraction. The values of Poisson's ratio for both the matrix and fibers are taken as 0.3, therefore effective values of  $\nu_{xy}$ ,  $\nu_{yz}$  and  $\nu_{xz}$  are found nearly same i.e. 0.3. **Figure 4.8** shows that the elastic modulus  $E_z$  decreases with the increase in the interior angle. **Figure 4.9** shows that the elastic moduli,  $E_x$  and  $E_y (E_x = E_y)$  increase with the increase in the interior angle. **Figure 4.10** shows the plots of maximum principal stress components for the unit-cell subjected to loading given in case-3 of **Table 4.2**. From these results, it is found that the stresses in yarns (fibers) are more than in the matrix region.



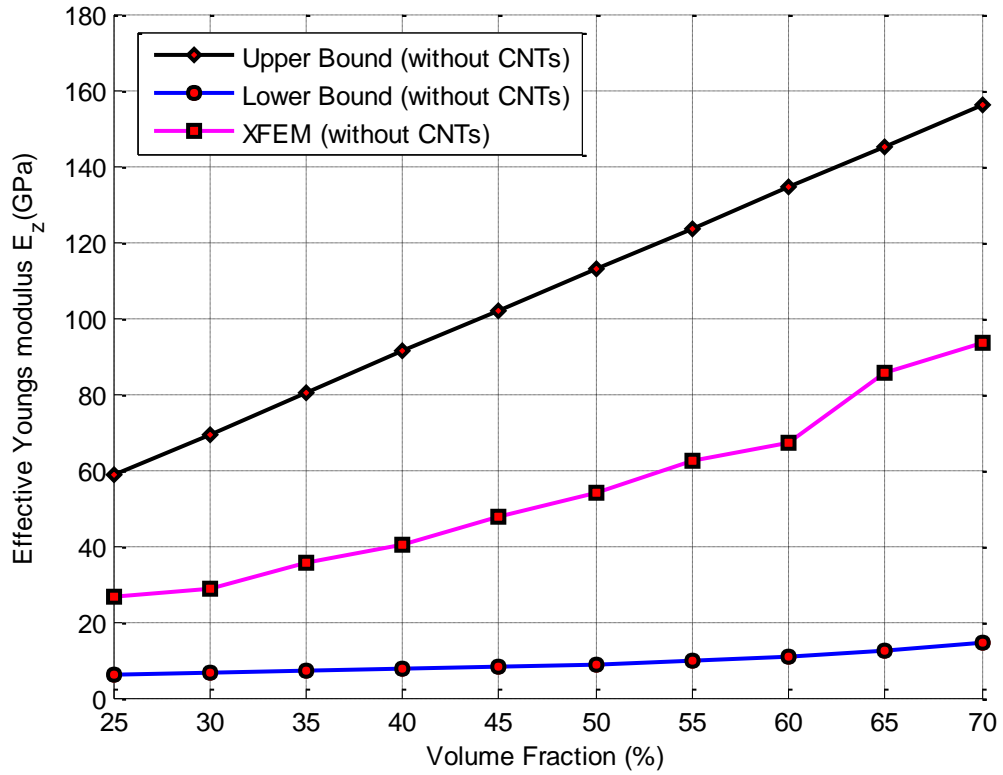


**Figure 4.4:** A plot of effective Young's modulus  $E_z$  with the fiber volume fraction

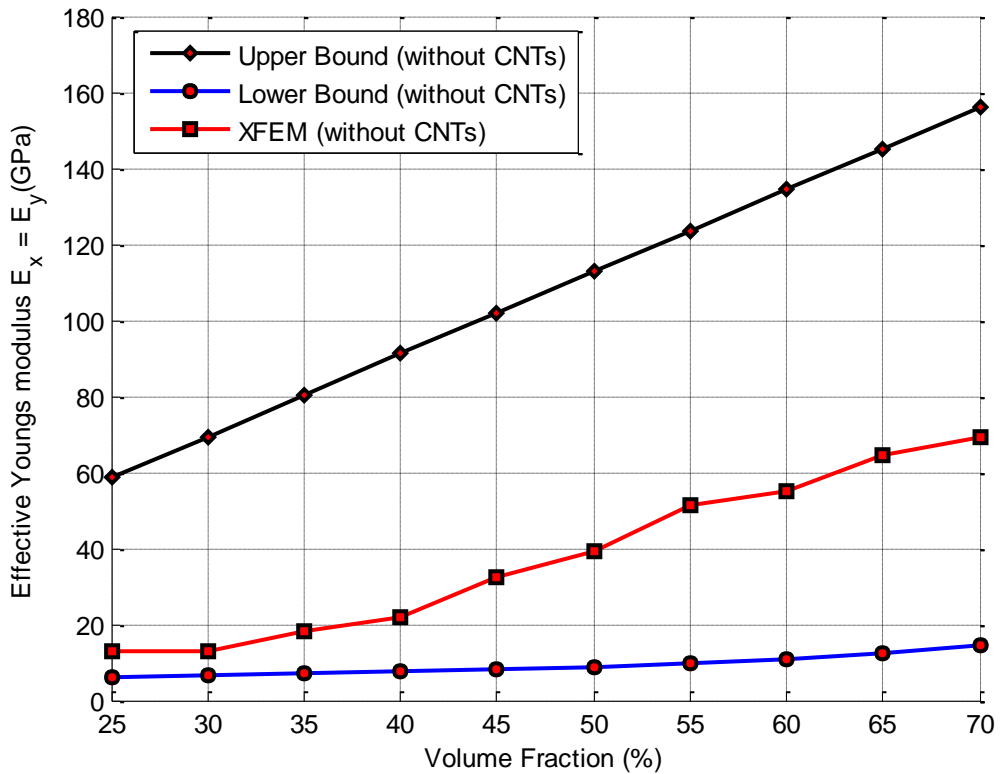


**Figure 4.5:** A plot of effective Young's modulus  $E_x$  and  $E_y$  ( $E_x = E_y$ ) with the fiber volume fraction

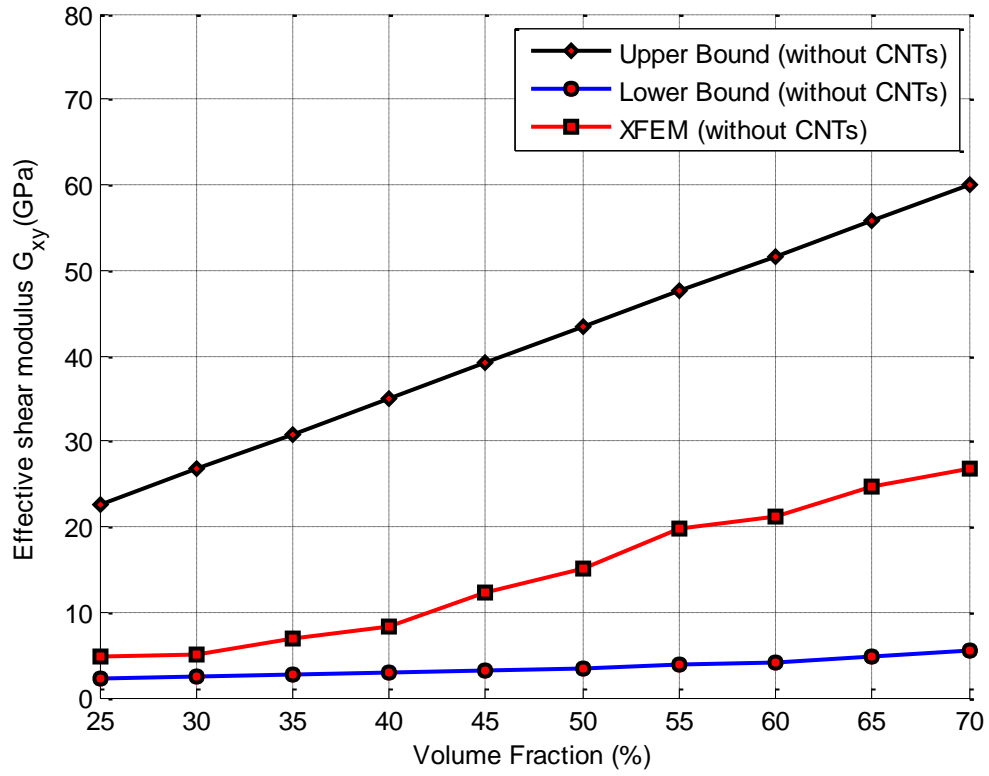


**Figure 4.6:** A plot of effective shear modulus  $G_{xy}$  with the fiber volume fraction

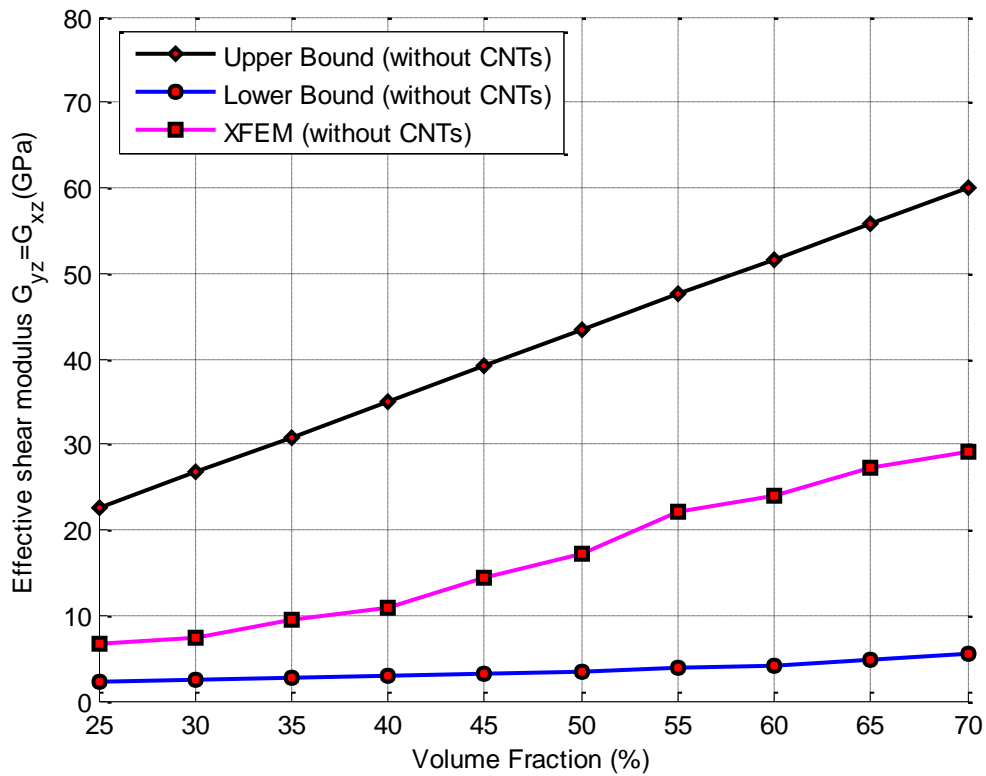


**Figure 4.7:** A plot of effective shear modulus  $G_{yz}$  and  $G_{xz}$  with the fiber volume fraction

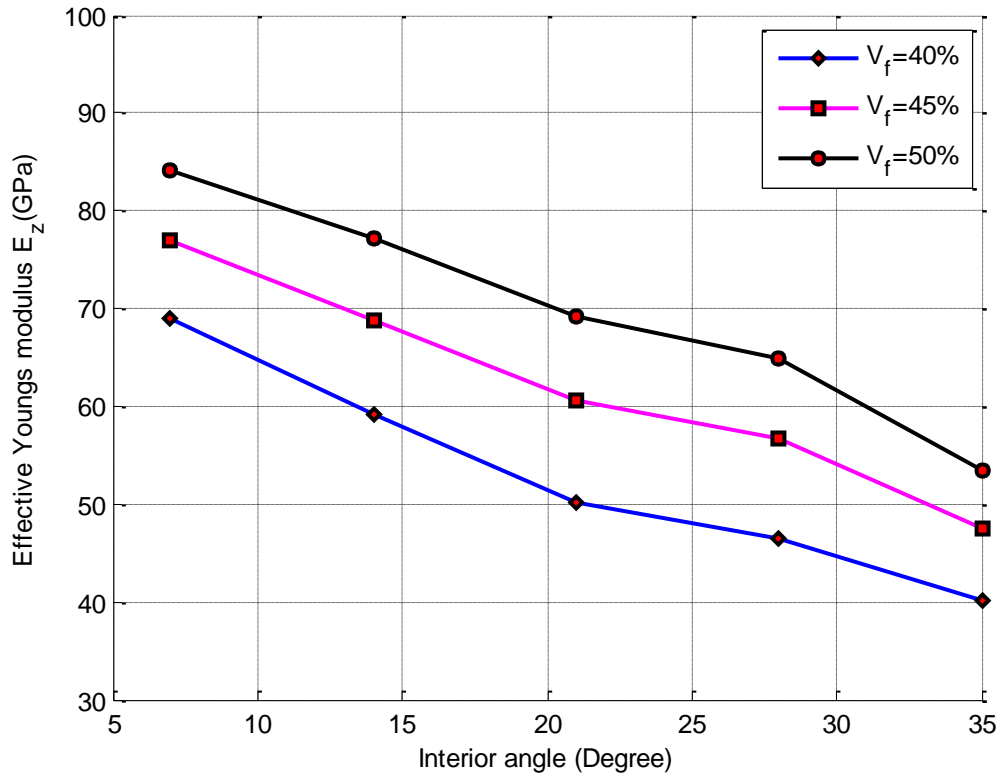


**Figure 4.8:** A plot of effective elastic modulus  $E_z$  with the interior angle

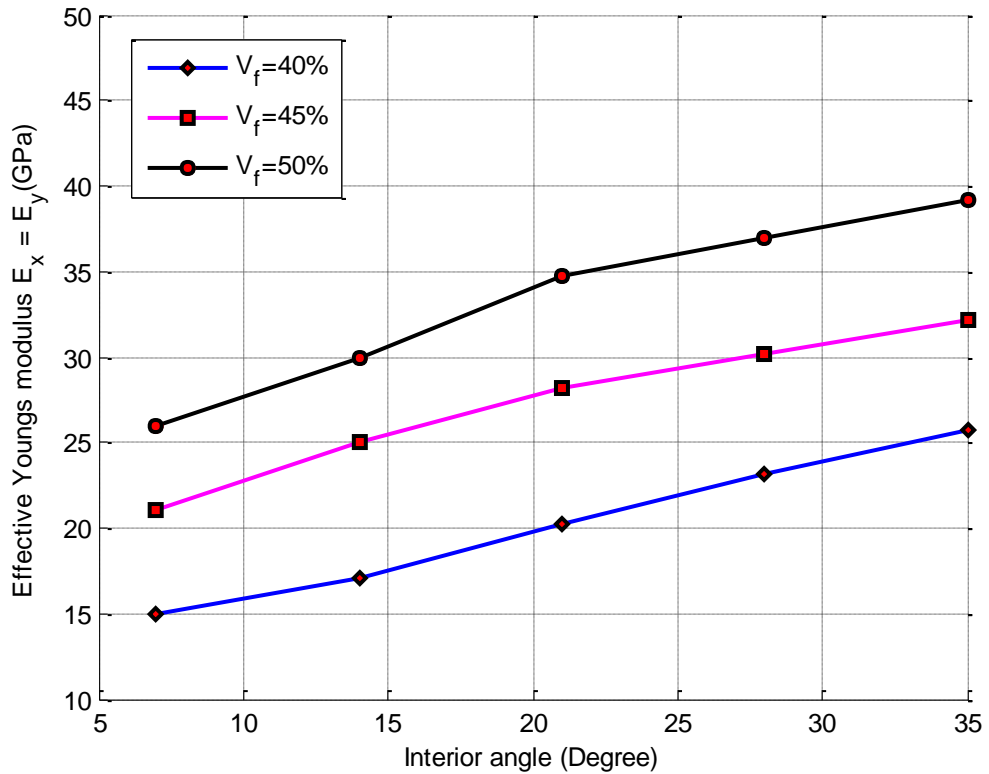


**Figure 4.9:** A plot of effective elastic modulus  $E_x$  and  $E_y$  ( $E_x = E_y$ ) with interior angle

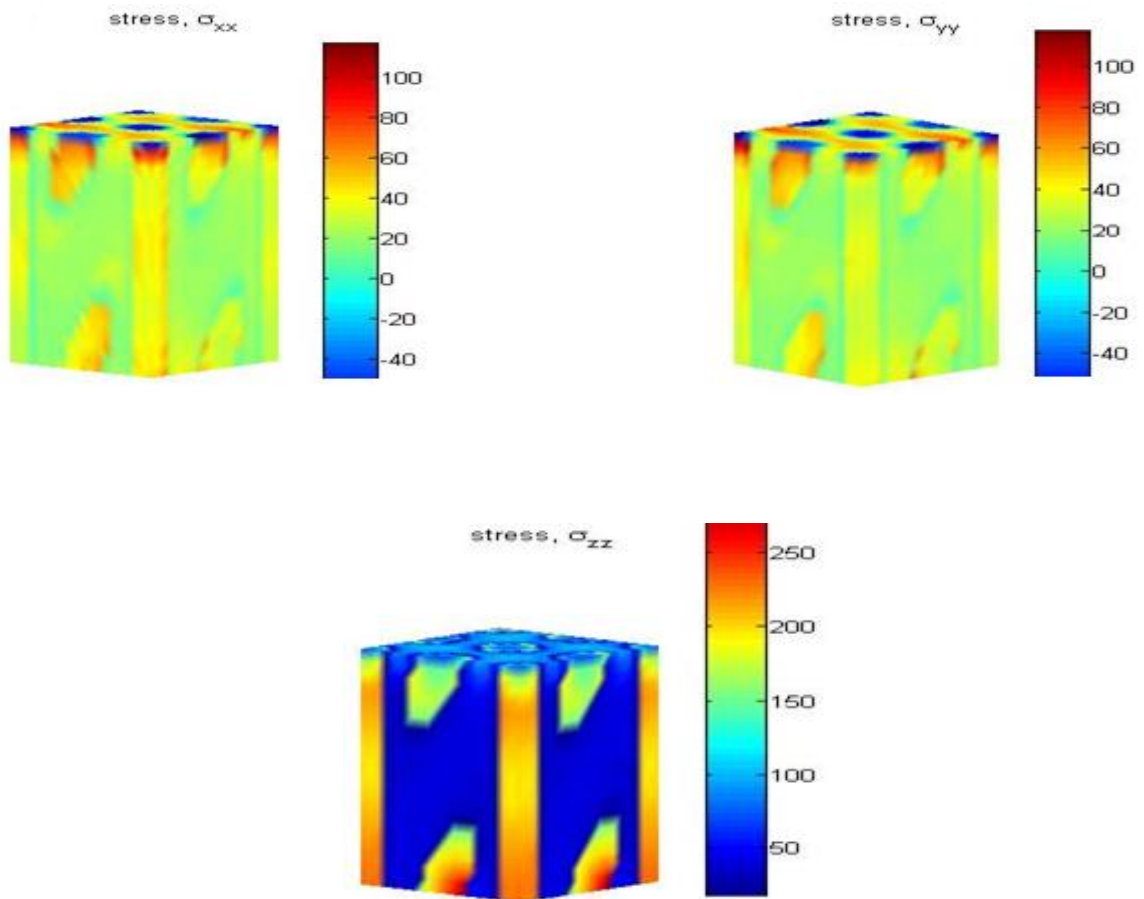


**Figure 4.10:** The plots of stress components  $\sigma_{xx}$ ,  $\sigma_{yy}$  and  $\sigma_{zz}$  for the unit-cell